NACA TN 3820

# NATIONAL ADVISORY COMMITTEE FOR AERONAUTICS

**TECHNICAL NOTE 3820**

## SOME OBSERVATIONS ON MAXIMUM PRESSURE RISE ACROSS SHOCKS WITHOUT BOUNDARY-LAYER SEPARATION ON AIRFOILS AT TRANSONIC SPEEDS

By Walter F. Lindsey and Patrick J. Johnston

Langley Aeronautical Laboratory
Langley Field, Va.

Washington
November 1956

NATIONAL ADVISORY COMMITTEE FOR AERONAUTICS

TECHNICAL NOTE 3820

# SOME OBSERVATIONS ON MAXIMUM PRESSURE RISE ACROSS SHOCKS WITHOUT BOUNDARY-LAYER SEPARATION ON AIRFOILS AT TRANSONIC SPEEDS

By Walter F. Lindsey and Patrick J. Johnston

## SUMMARY

An investigation of the two-dimensional flow along flat plates having rounded leading edges has provided additional information on shock-induced separation. The results indicate that laminar boundary layers can sustain the theoretical pressure rise for normal shocks without separating provided that the local Mach numbers are less than about 1.4. The permissible pressure rise across shocks without boundary-layer separation on rounded-leading-edge airfoils having flat sides or convex surfaces was observed to increase with increase in angle of attack and proximity of shock to airfoil leading edge.

## INTRODUCTION

There is much work available concerning the details of an established separated flow in the presence of compression shocks. (For example, refs. 1, 2, 3, and 4.) Other investigators have shown the detrimental effects of flow separation, not only on steady-state (time-average) flow conditions but also on unsteady force characteristics. (See refs. 5, 6, and 7.) A better understanding of factors affecting separation is therefore needed in order to evaluate the changes required to alleviate the separation, particularly on airfoils at transonic speeds.

Investigations on airfoils (refs. 8 and 9) and in nozzles (ref. 10) have shown that the surface pressure rise through a shock is less than the theoretical value. Channel-flow studies (ref. 11) indicated that the surface pressure rise across the shock was modified by boundary layers so that the theoretical rise was not obtained. Later investigators (refs. 12 and 13) supported the experimental results of reference 11.

Some recent measurements of the pressure distributions on two-dimensional flat plates having rounded leading edges showed pressure

rises through shocks that corresponded to theoretical normal-shock values. Information of this type at transonic speeds is useful in estimating the maximum oscillating panel loads on wings, as well as providing additional data concerning effects of shock on boundary layer. These transonic data have been studied and the results are presented herein.

## SYMBOLS

| | |
|---|---|
| $M$ | free-stream Mach number |
| $M_1$ | Mach number at static-pressure orifice on model immediately upstream of shock |
| $M_2$ | Mach number at static-pressure orifice on model immediately downstream of shock |
| $M_l$ | local Mach number |
| $p$ | free-stream static pressure |
| $p_1$ | static pressure at static-pressure orifice on model immediately upstream of shock |
| $p_2$ | static pressure at static-pressure orifice on model immediately downstream of shock |
| $p_l$ | local static pressure |
| $q$ | free-stream dynamic pressure |
| $\Delta p$ | pressure increment across shock wave, $p_2 - p_1$ |
| $x$ | distance along chord |
| $\alpha$ | angle of attack, deg |

## APPARATUS AND TESTS

Tests on flat plates having rounded leading edges were conducted in the Langley 4- by 19-inch semiopen tunnel operating as a direct blowdown tunnel from a supply of dry compressed air. (See fig. 1.) The tunnel test section was open along the top and bottom boundaries,

and the chambers extending beyond those two boundaries were connected by a duct. The test region and the calibration of the flow are as described in reference 14.

Each model had a 4-inch chord and completely spanned the 4-inch dimension of the tunnel. The models were mounted in circular end plates which maintained the continuity of the tunnel walls. The profiles were two-percent-thick flat plates and had rounded leading and trailing edges corresponding to various combinations of elliptical shapes with fineness ratios of 0, 1, 4, and 10. The models are designated as "a-b," where "a" is the fineness ratio of the leading edge and "b" is the similar notation for the trailing edge. For the present investigation, however, the trailing-edge shape has no significant effect and is neglected by designating it as "X."

Data were obtained from schlieren photographs of the flow and pressure measurements along the surfaces of the models. The surface pressure measurements were obtained by means of 44 static-pressure orifices installed in the surfaces of the models and connected to a manometer so that the distribution of pressure along the surfaces could be recorded. Pictures of the flows were taken over the speed range at $0^\circ$ angle of attack by using a 35-millimeter motion-picture camera and the technique described in reference 15. Since each picture had an exposure of 4 microseconds, individual frames were selected as still photographs. The Mach number range of the tests extended from 0.70 to 1.0, and the corresponding Reynolds number range was from $1.8 \times 10^6$ to $2.1 \times 10^6$, based on the 4-inch chord of the models.

## DISCUSSION

### Flat Plates

The variation of static pressures along the surfaces of flat plates at $0^\circ$ angle of attack from the present tests, presented in figure 2, indicates that the changes in pressure in the vicinity of compression shocks (flagged symbols) are very large. The data in figure 2 show that the trailing-edge shape has no effect on the flows involved in this discussion and is designated hereafter as "X."

Schlieren photographs of the flow past these models were obtained and are presented in figure 3 for "a-X" airfoils. The photographs and a study of the motion pictures of the flow past each of the two surfaces of the models ($\alpha = 0^\circ$) showed for the range of Mach numbers in figures 2 and 3 (0.851 to 0.975) that the flow, in general, was unseparated at the shock. However, random occurrences of flow separation under the shock were observed; therefore it is indicated that the flow was verging on the condition for separation. (See, for example, the flow past the upper surface of the 4-X airfoil at a Mach number of 0.858 in fig. 3.)

As the free-stream Mach number was increased beyond the values in figures 2 and 3 and approached 1.0, the shock moved rearward and approached the trailing edge. The pressure rise across shock became obscured at these high Mach numbers through a thickening of the boundary layer or flow separation. The flows presented in figures 2 and 3 represent the approximate limiting conditions for unseparated flow.

The flow in the schlieren photographs of figure 3 appeared to be laminar ahead of the shock and generally became turbulent downstream of the shock. The flow could be expected to be laminar ahead of the shock because of the low Reynolds number of the flow in this region. Furthermore, previous experience in this tunnel, during investigations on two-dimensional airfoils, with and without forced transition or roughness strips, provided additional evidence of this observation.

The maximum pressure rise across the shocks without boundary-layer separation, obtained from the flagged symbols in figure 2, is presented in figure 4 as a function of the shock location. The curves in figure 4 are envelope curves of the maximum values for each of the three flat plates. The data show that the pressure rise decreases as the shock moves rearward along the airfoil surface. The rearward movement of the shock is accompanied with a growth in the boundary-layer thickness and a decrease in the Mach number upstream of the shock. The decrease in Mach number upstream of the shock is accompanied with a decrease in the theoretical pressure rise, and the shock adjusts its position along the flat plates so that the flow is verging on separation for the data presented.

The decrease in pressure rise associated with rearward movement of the shock is similar to the effect of increasing Reynolds number on the pressure rise for separation of a laminar boundary layer observed in the case of supersonic flow. These data also show that an increase in leading-edge bluntness is accompanied with an increase in permissible pressure recovery across shock at any given chordwise location.

Since an increase in leading-edge radius and an increase in angle of attack produce increases in the maximum induced velocity, it was of interest to examine data at a higher angle of attack to see whether these effects of leading-edge radius or bluntness would be produced also by increasing the angle of attack. Pressure-distribution data at $2^{\circ}$ and $4^{\circ}$ angles of attack were examined. Data for unseparated flow, similar to those in figure 4, were obtained from the pressure distributions at $2^{\circ}$, and a comparison of the data at an angle of attack of $0^{\circ}$ and $2^{\circ}$ is presented in figure 5. The results indicate that at low angles of attack an increase in angle of attack is accompanied with an increase in the obtainable pressure recovery. The results, furthermore, indicate a maximum pressure ratio that can be sustained by the boundary layer before separation, inasmuch as both the most blunt and the medium blunt nose (1-X and 4-X) have the same values of pressure rise at an angle of attack of $2^{\circ}$.

The maximum pressure rise that the boundary layer can sustain across the shock without separation of the flow was obtained from figure 2 at an angle of attack of $0^{\circ}$ and from similar data at an angle of attack of $2^{\circ}$. These data are plotted in figure 6 as a function of the Mach number in front of shock and are compared with the theoretical pressure recovery for normal shocks. Although Mach numbers greater than 1.35 ahead of the shock were observed in the tests, a Mach number of about 1.35 appears to be the limit for the occurrence of unseparated flow and, consequently, is the upper limit for agreement between theoretical and experimental pressure recoveries across the shock for these tests. Similar agreement between theory and experiment has been shown by some early investigators (ref. 8) to occur only in the flow field above the test model. Those flow-field results were measured at orifices in a static-pressure probe on which a laminar boundary layer would be expected to exist. Those measurements therefore can be considered to substantiate the data in figure 5.

The pressure rises across shocks presented in figures 2 to 6 are for transonic flows past flat plates without utilizing artificial means of producing separation. In reference 4 and others, a purely supersonic flow is forced to separate, and the pressure rises are measured between various selected positions within the separated flow. (See ref. 16.) The supersonic pressure recoveries in established separated flows are not comparable with the transonic shock-pressure recoveries for unseparated flows presented herein. In other words, the measured pressure rise across shocks in a separated flow is less than the rise before separation occurs, as indicated by references 1 and 16 and by an analysis of transonic airfoil data in reference 14.

## Airfoils

The results for the flat plates have shown that, as a shock moves rearward, the maximum pressure ratio for shock without separation decreases. On convex airfoils, however, the surface curvature is conducive to continuous increases in Mach number as the shock moves rearward. A rearward moving shock is accompanied with increases in shock strength and boundary-layer thickness and in the tendency of the flow to separate. As the free-stream Mach number is increased towards 1.0 and the shock moves rearward along the convex surface of an airfoil at a fixed attitude, transition from unseparated to separated flow might be expected to occur at one point in the speed range. Hence, data for the condition of imminent separation are very difficult to isolate from existing airfoil data because of the discrete Mach number intervals between test points.

A typical variation in the flow past an airfoil from existing data is shown in figures 7 and 8 (from investigation reported in ref. 9).

The data shown in figure 7 bracket, but do not isolate, the actual conditions of flow separation on the model surface. The data show the variation in local Mach number (based on local static pressure and free-stream total pressure) along the chord as affected by changes in the free-stream Mach number. At a free-stream Mach number between 0.680 and 0.707, a measured Mach number immediately upstream of the shock $M_1$ between 1.1 and 1.18 is observed and is followed by a very rapid pressure rise that reduces the local measured Mach number downstream of shock $M_2$ to values less than sonic velocity on the upper surface. The decrease roughly approximates that for a normal shock.

As the free-stream Mach number M is increased, the local Mach number $M_l$ also increases and laminar separation occurs. The laminar separation is indicated by the region of near-zero pressure gradient ahead of the shock, and the chordwise extent of the separation increases with rearward movement of the shock. (See also fig. 8.) The rearward shock movement is also accompanied with the continuous smoothing out of the abruptness of the transition from a steep pressure gradient to a more normal gradient along the airfoil surface at the rear of the discontinuity. When the shock is moved well back on the airfoil, a smoothing of this pressure transition region also occurs ahead of the shock and is probably associated with a change from laminar separation to turbulent separation of large magnitude. (See fig. 8.) The flow on the lower surface is very similar. (See figs. 7(b) and 8.)

A large amount of data from investigations reported in references 9 and 14 were examined and points were chosen to correspond to the flows represented in figure 7 at Mach numbers between 0.680 and 0.707 for the upper surface and around 0.767 on the lower surface. The pressure rises obtained, expressed in terms of the pressure upstream of the shock, are presented in figure 9 as a function of the position of the shock x for a variety of airfoils and are compared with the measured pressure rises across the shocks without separation on the flat plates at an angle of attack of $2^\circ$. The data for the NACA 64A009 airfoil provided information at various angles of attack and showed that the pressure rise without flow separation increases with increase in the angle of attack. This result is in good agreement with the data on the flat plates. The increased slope of the data for the NACA 64A009 airfoil, however, is a result of the cumulative effects of increasing angle of attack and decreasing distance from the leading edge to position of shock.

The pressure rises for the convex airfoils are presented as a function of the local Mach number immediately upstream of the shock $M_1$ in figure 10. The agreement of the data with the theoretical normal-shock values is similar to that observed for the flat plates in figure 6. The general agreement in the existence of a maximum local Mach number of slightly below 1.4 for unseparated flow, not only from the present investigation concerning laminar boundary layers but also from previous

investigations (for example, ref. 17 and discussion of Fage and Sargent's work in ref. 1) for turbulent flow, indicates that at transonic speeds the maximum pressure rise without flow separation may not be too strongly influenced by the type of boundary layer on the surface.

## CONCLUDING REMARKS

An investigation at transonic speeds of the flow along flat plates having rounded leading edges has provided additional information on shock-induced separation. The maximum observed pressure rise across shocks for laminar boundary layers without separating on rounded-leading-edge airfoils having flat sides or convex surfaces increases with increase in angle of attack and proximity of shock to airfoil leading edge.

The general agreement in the existence of a maximum local Mach number of somewhat below 1.4 for the occurrence of unseparated flow, not only from the present investigation involving laminar boundary layers but also from investigations for turbulent flow, indicates that at transonic speeds the maximum pressure rise obtainable without separation may not be too strongly influenced by the type of the boundary layer on the surface.

Langley Aeronautical Laboratory,
National Advisory Committee for Aeronautics,
Langley Field, Va., July 23, 1956.

## REFERENCES

1. Holder, D. W., Pearcey, H. H., and Gadd, G. E.: The Interaction Between Shock Waves and Boundary Layers, with a note on "The Effects of the Interaction on the Performance of Supersonic Intakes," by J. Seddon. C.P. No. 180, British A.R.C., 1955.

2. Bogdonoff, S. M., Kepler, C. E., and Sanlorenzo, E.: A Study of Shock Wave Turbulent Boundary Layer Interaction at M = 3. Rep. No. 222 (Contract No. N6-onr-270, Task Order No. 6, Project Number NR-061-049), Dept. Aero. Eng., Princeton Univ., July 1953.

3. Allen, H. Julian, Heaslet, Max. A., and Nitzberg, Gerald E.: The Interaction of Boundary Layer and Compression Shock and Its Effect Upon Airfoil Pressure Distributions. NACA RM A7A02, 1947.

4. Lange, Roy H.: Present Status of Information Relative to the Prediction of Shock-Induced Boundary-Layer Separation. NACA TN 3065, 1954.

5. Daley, Bernard N., and Humphreys, Milton D.: Effects of Compressibility on the Flow Past Thick Airfoil Sections. NACA TN 1657, 1948.

6. Humphreys, Milton D.: Pressure Pulsations on Rigid Airfoils at Transonic Speeds. NACA RM L51I12, 1951.

7. Humphreys, Milton D., and Kent, John D.: The Effects of Camber and Leading-Edge-Flap Deflection on the Pressure Pulsations on Thin Rigid Airfoils at Transonic Speeds. NACA RM L52G22, 1952.

8. Stack, John, Lindsey, W. F., and Littell, Robert E.: The Compressibility Burble and the Effect of Compressibility on Pressures and Forces Acting on an Airfoil. NACA Rep. 646, 1938.

9. Daley, Bernard N.: Effects of Compressibility on the Characteristics of Five Airfoils. NACA RM L6L16, 1947.

10. Donaldson, Coleman duP.: Effects of Interaction Between Normal Shock and Boundary Layer. NACA CB 4A27, 1944.

11. Ackeret, J., Feldmann, F., and Rott, N.: Investigations of Compression Shocks and Boundary Layers in Gases Moving at High Speed. NACA TM 1113, 1947.

12. Liepmann, H. W., Roshko, A., and Dhawan, S.: On Reflection of Shock Waves From Boundary Layers. NACA Rep. 1100, 1952. (Supersedes NACA TN 2334.)

13. Wood, George P., and Gooderum, Paul B.: Investigation With an Interferometer of the Flow Around a Circular-Arc Airfoil at Mach Numbers Between 0.6 and 0.9. NACA TN 2801, 1952.

14. Daley, Bernard N., and Dick, Richard S.: Effect of Thickness, Camber, and Thickness Distribution on Airfoil Characteristics at Mach Numbers Up to 1.0. NACA TN 3607, 1956. (Supersedes NACA RM L52G31a.)

15. Lindsey, Walter F., and Burlock, Joseph.: A Variable-Frequency Light Synchronized With a High-Speed Motion-Picture Camera to Provide Very Short Exposure Times. NACA TN 2949, 1953.

16. Love, Eugene S.: Pressure Rise Associated With Shock-Induced Boundary-Layer Separation. NACA TN 3601, 1955.

17. Nussdorfer, T. J.: Some Oberservations of Shock-Induced Turbulent Separation on Supersonic Diffusers. NACA RM E51L26, 1954.

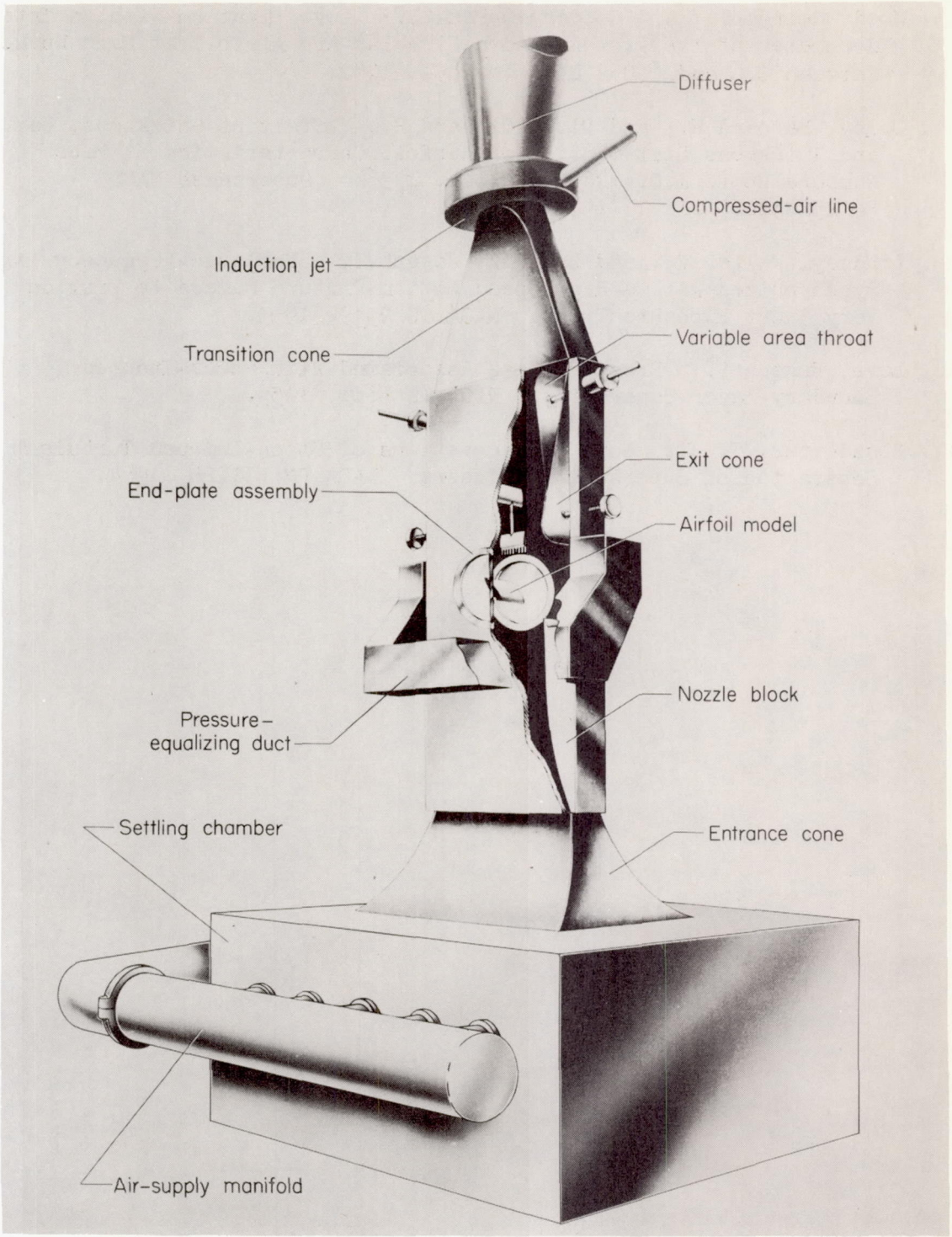


L-83293.1

Figure 1.- Langley 4- by 19-inch semiopen blowdown tunnel.

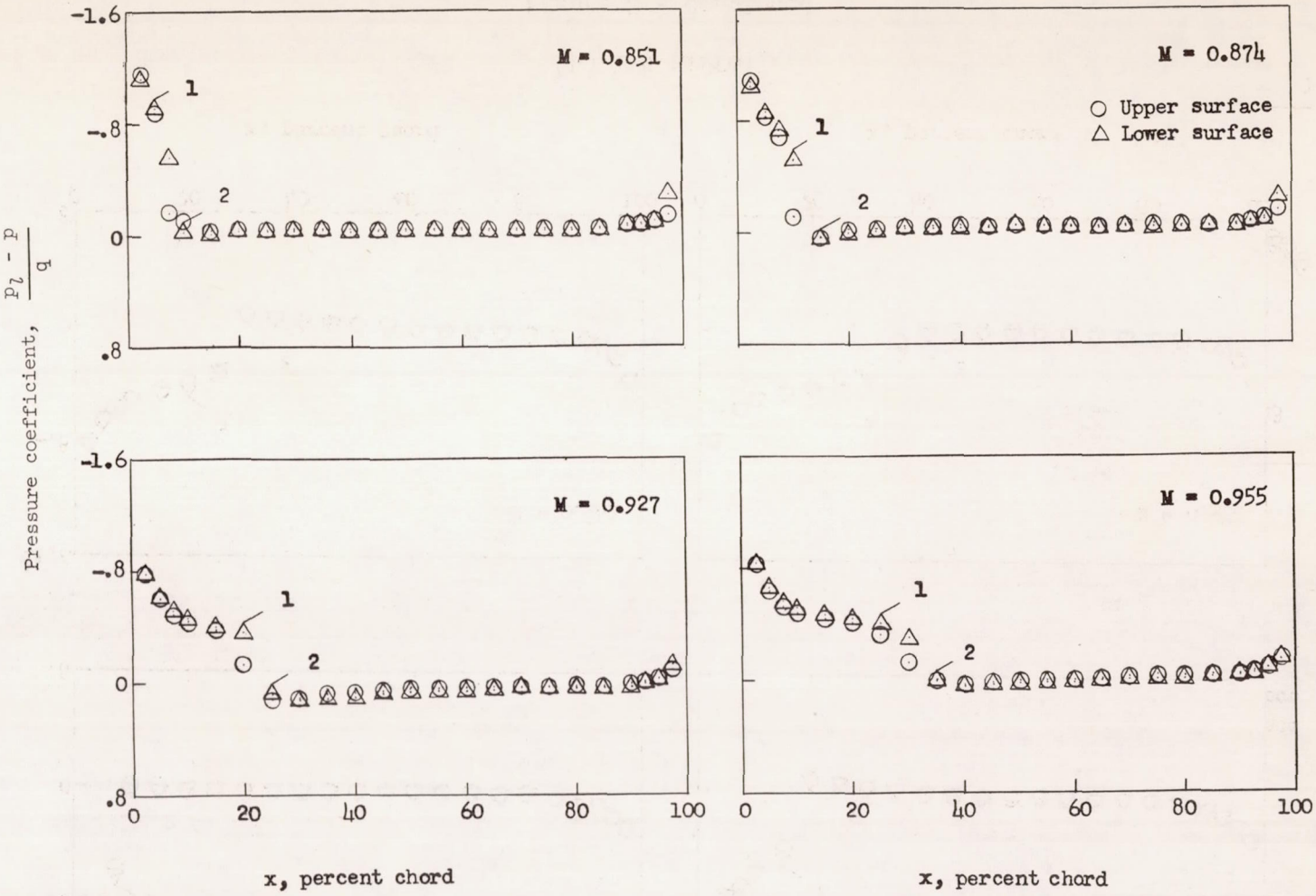


(a) 1-0 airfoil.

Figure 2.- Pressure distributions along surfaces of flat plates having rounded edges; $\alpha = 0^\circ$.

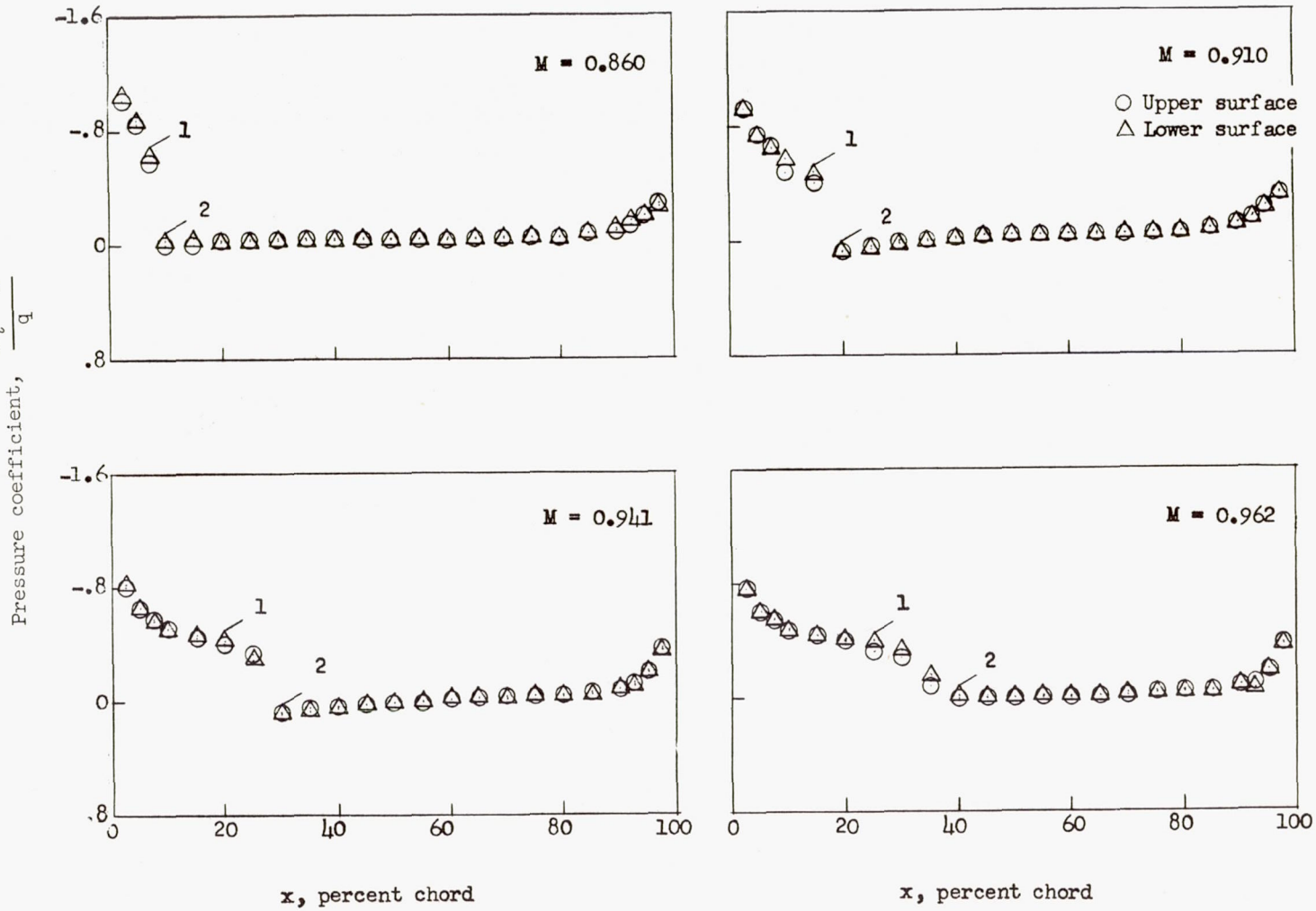


(b) 1-4 airfoil.

Figure 2.- Continued.

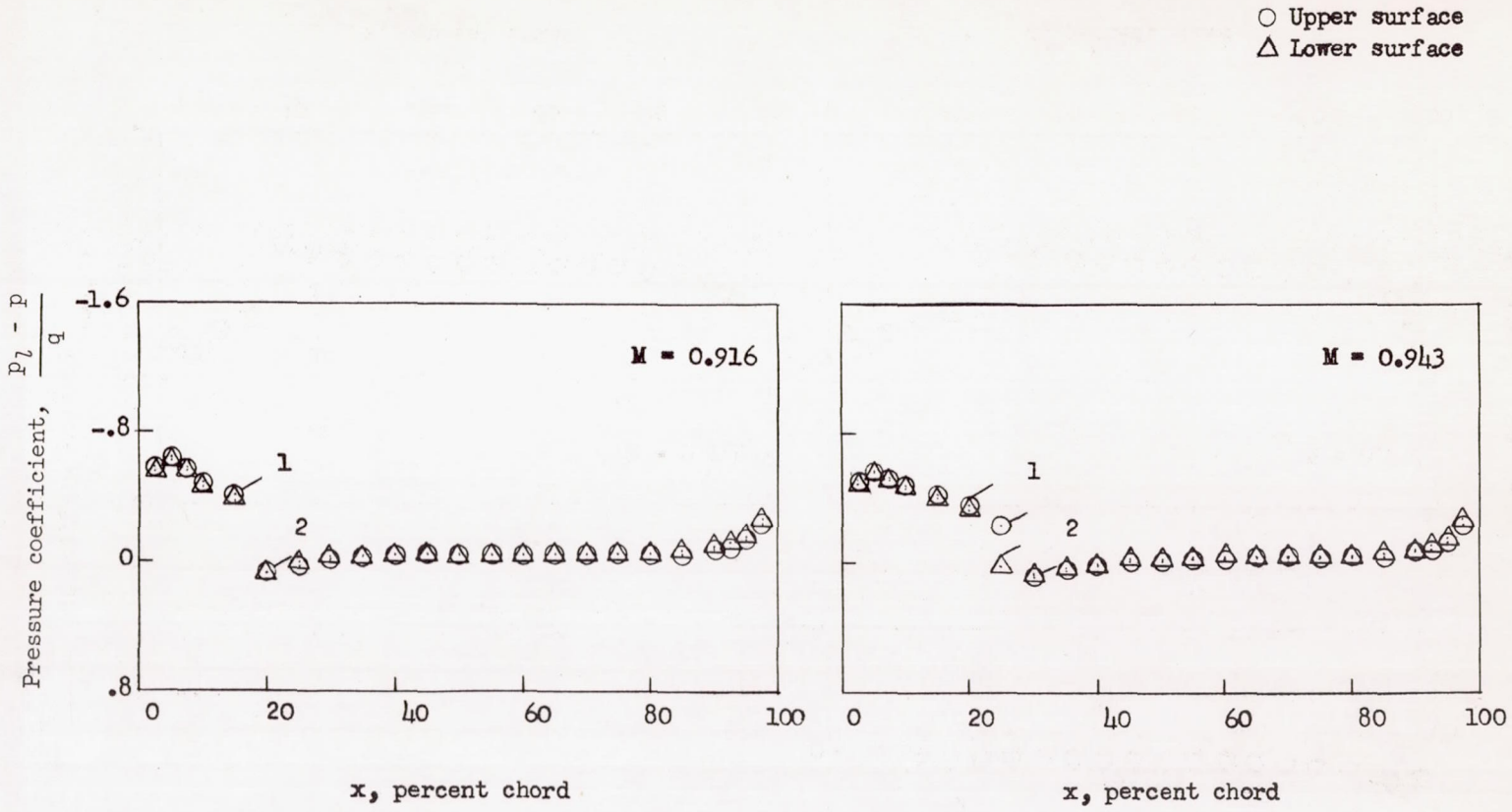


(c) 4-1 airfoil.

Figure 2.- Continued.

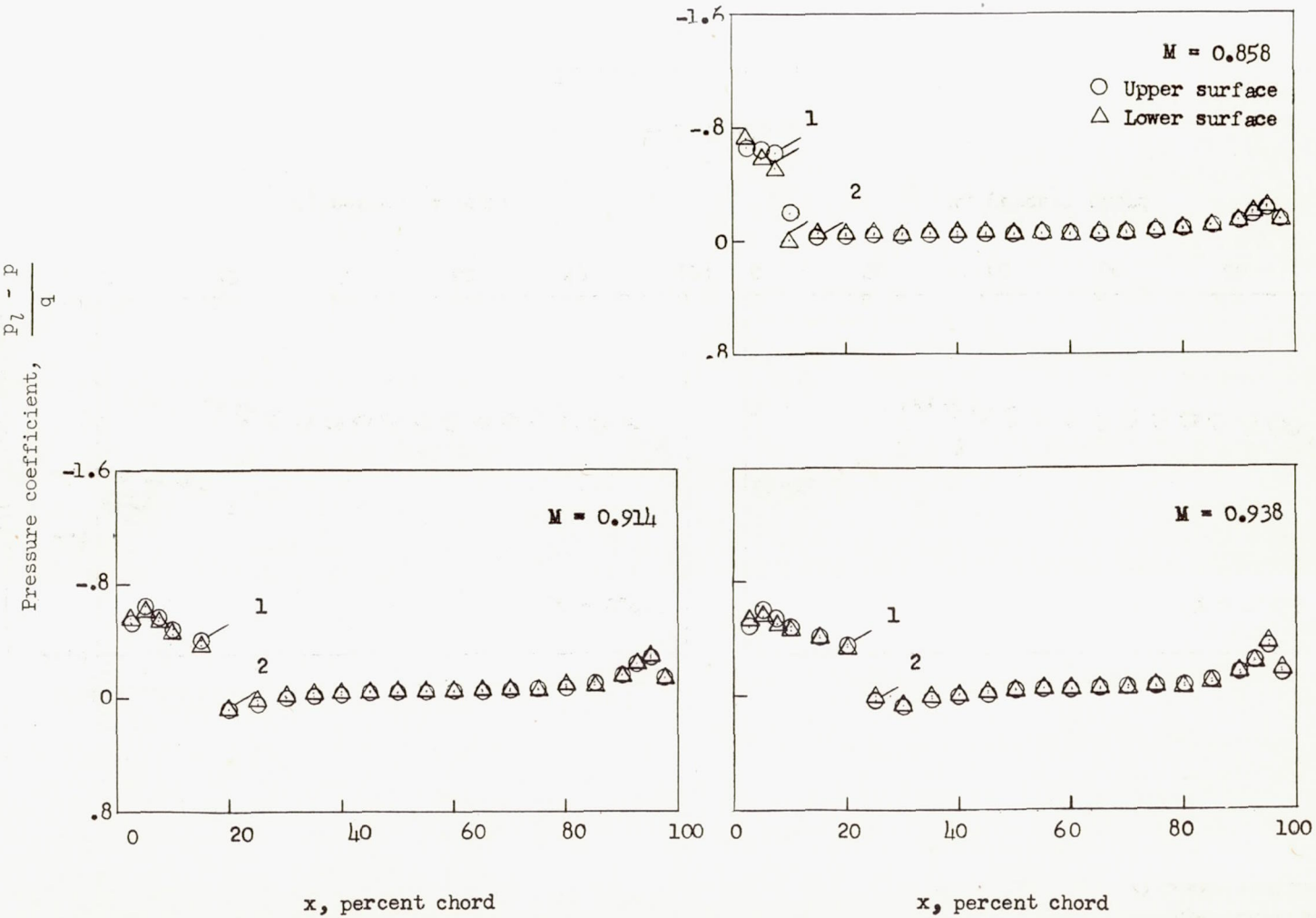


(d) 4-10 airfoil.

Figure 2.- Continued.

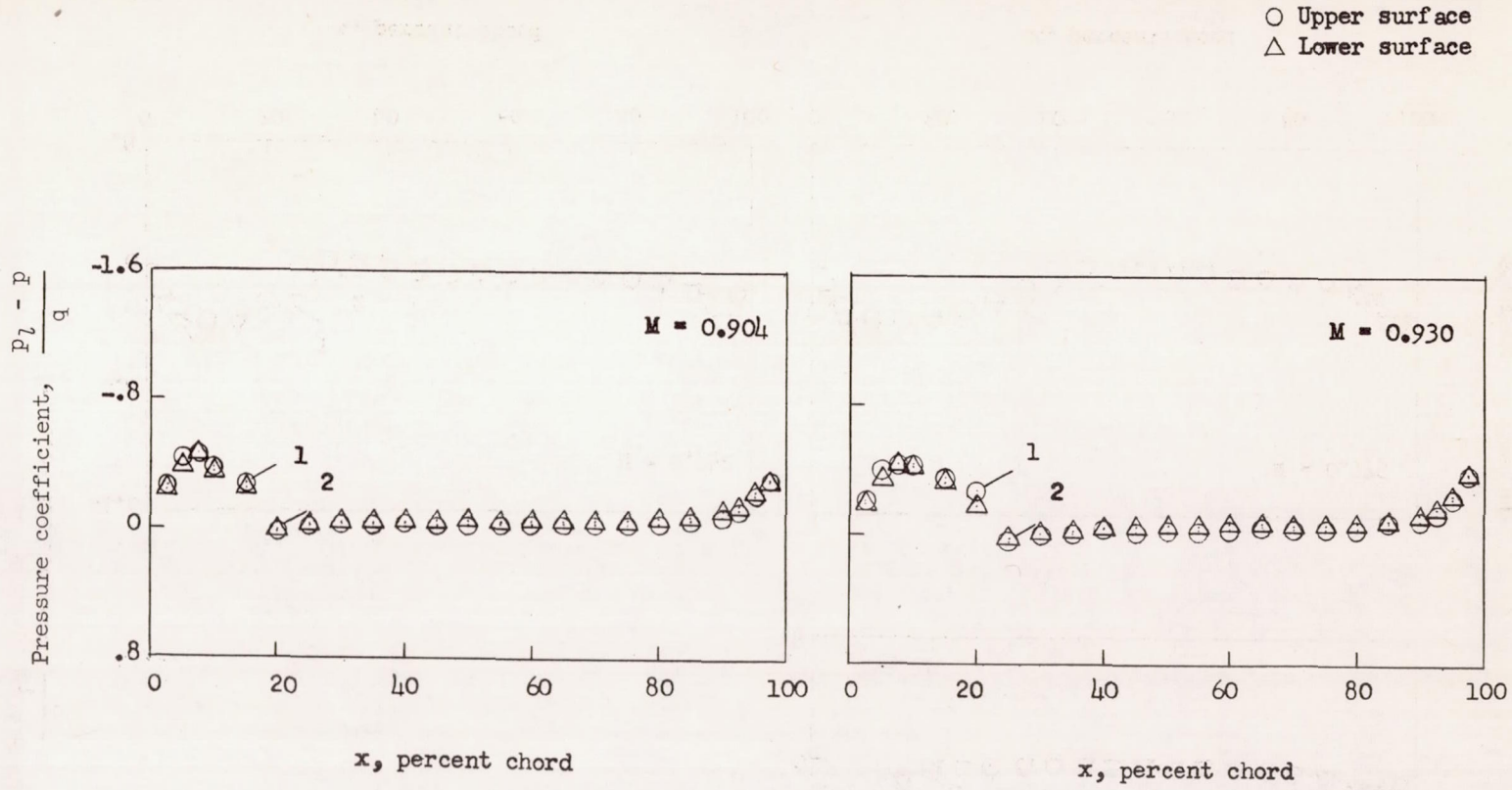


(e) 10-4 airfoil.

Figure 2.- Continued.

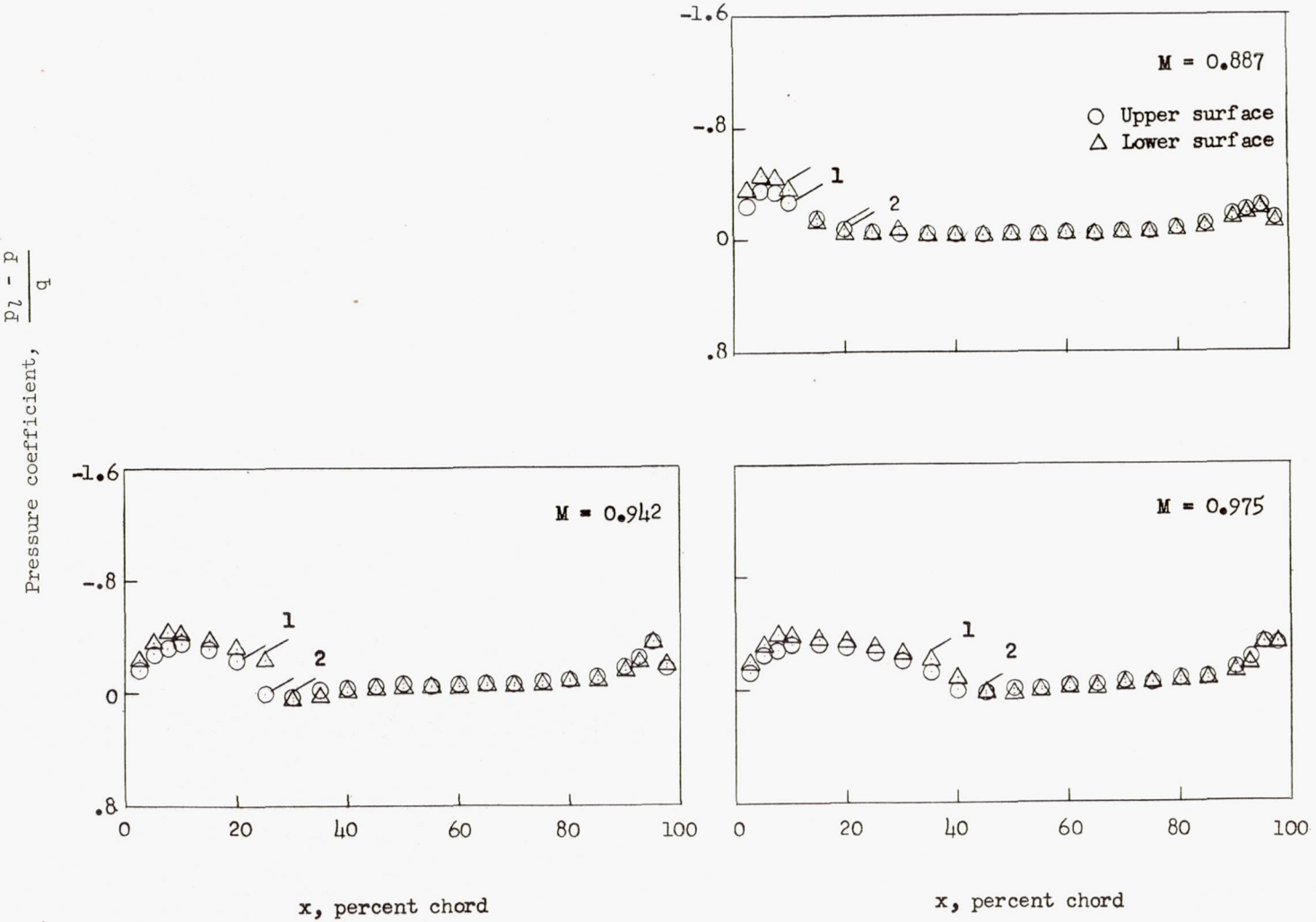


(f) 10-10 airfoil.

Figure 2.- Concluded.

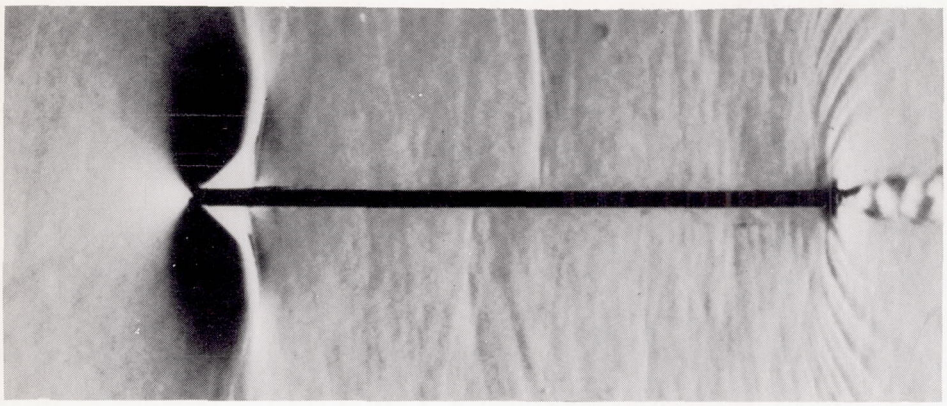

THE 1-X PROFILE, M = 0.851

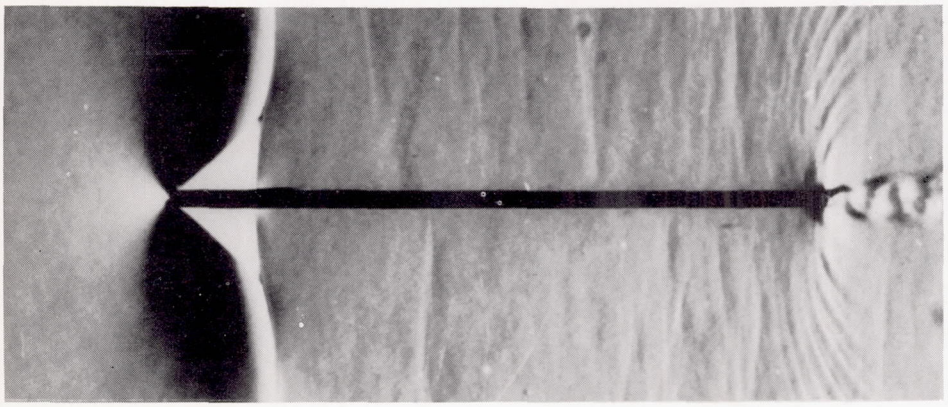

THE 1-X PROFILE, M = 0.874

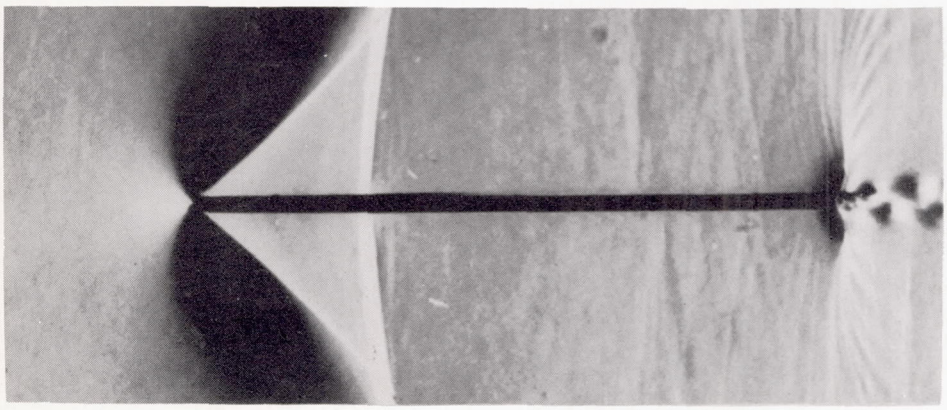

THE 1-X PROFILE, M = 0.927

L-93585

Figure 3.- Flow past the 2-percent-thick flat plates.

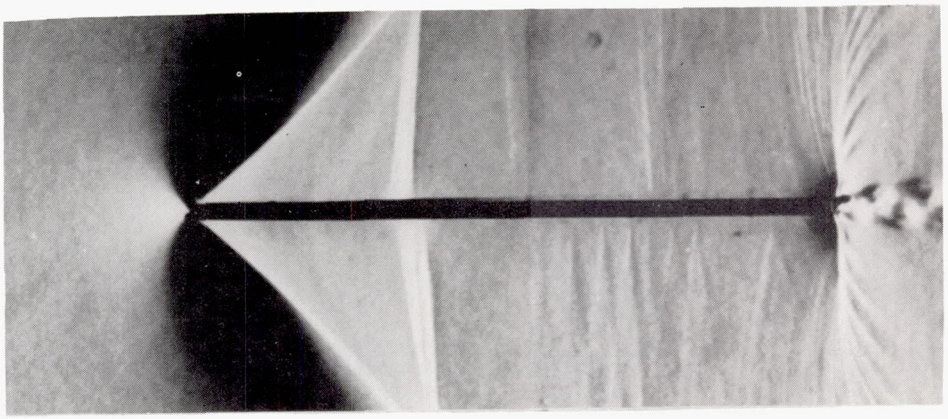

THE 1-X PROFILE, M = 0.955

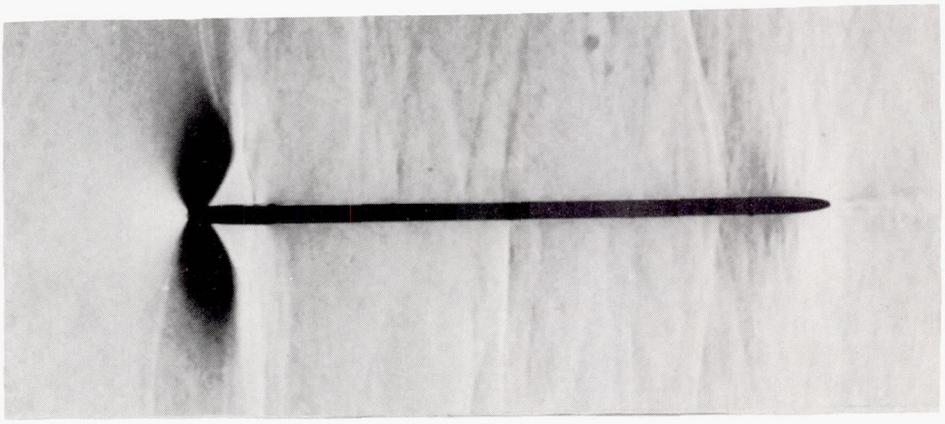

THE 4-X PROFILE, M = 0.858

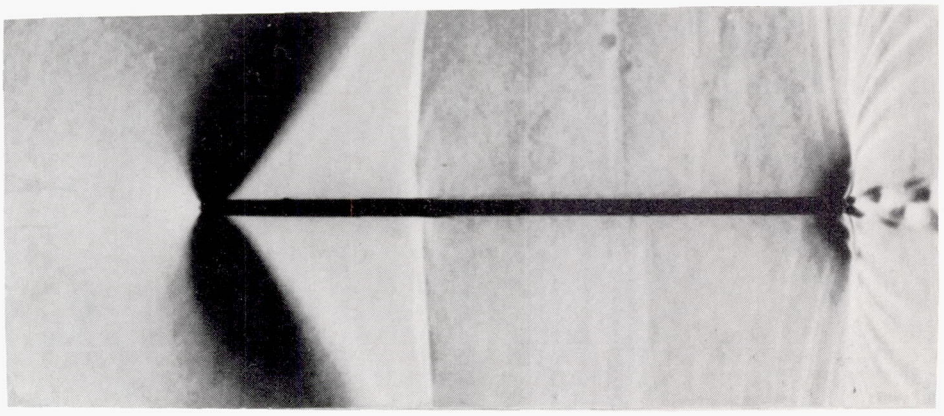

THE 4-X PROFILE, M = 0.943

L-93586

Figure 3.- Continued.

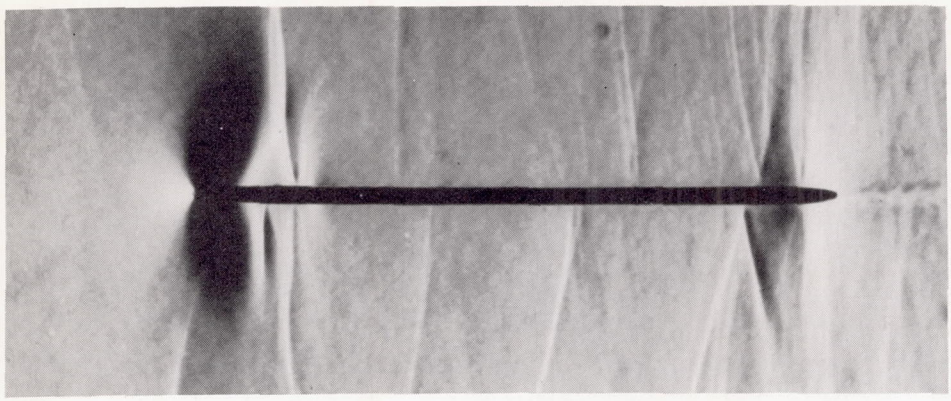

THE 10-X PROFILE, M = 0.887

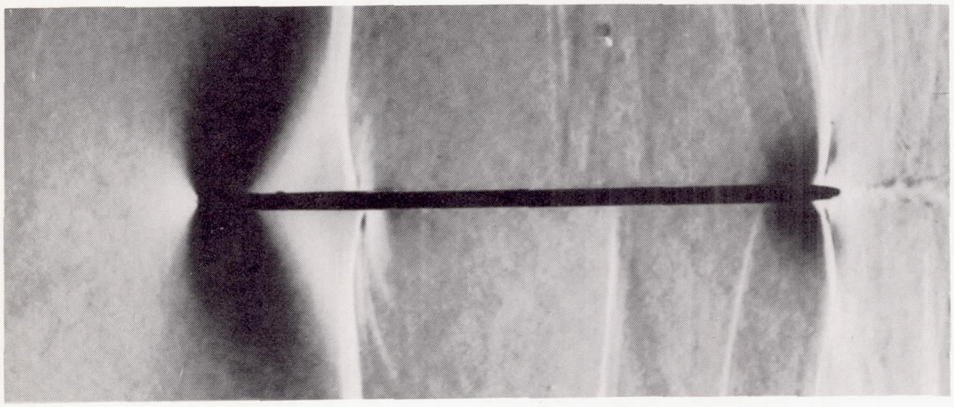

THE 10-X PROFILE, M = 0.942

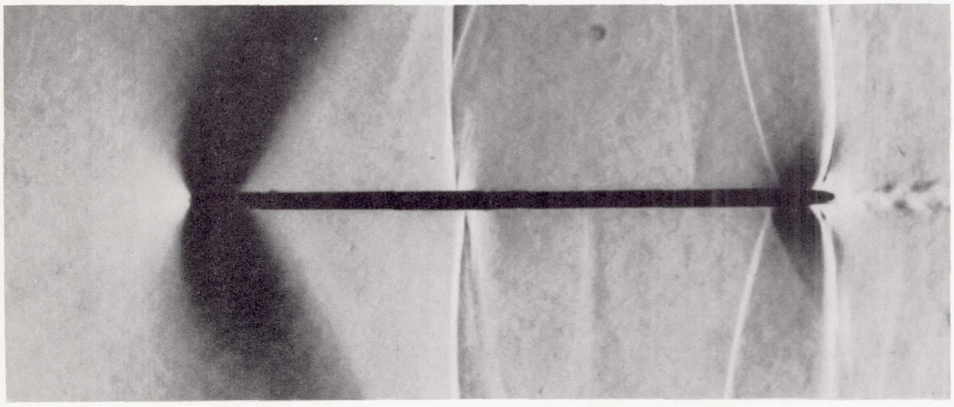

THE 10-X PROFILE, M = 0.975

L-93587

Figure 3.- Concluded.

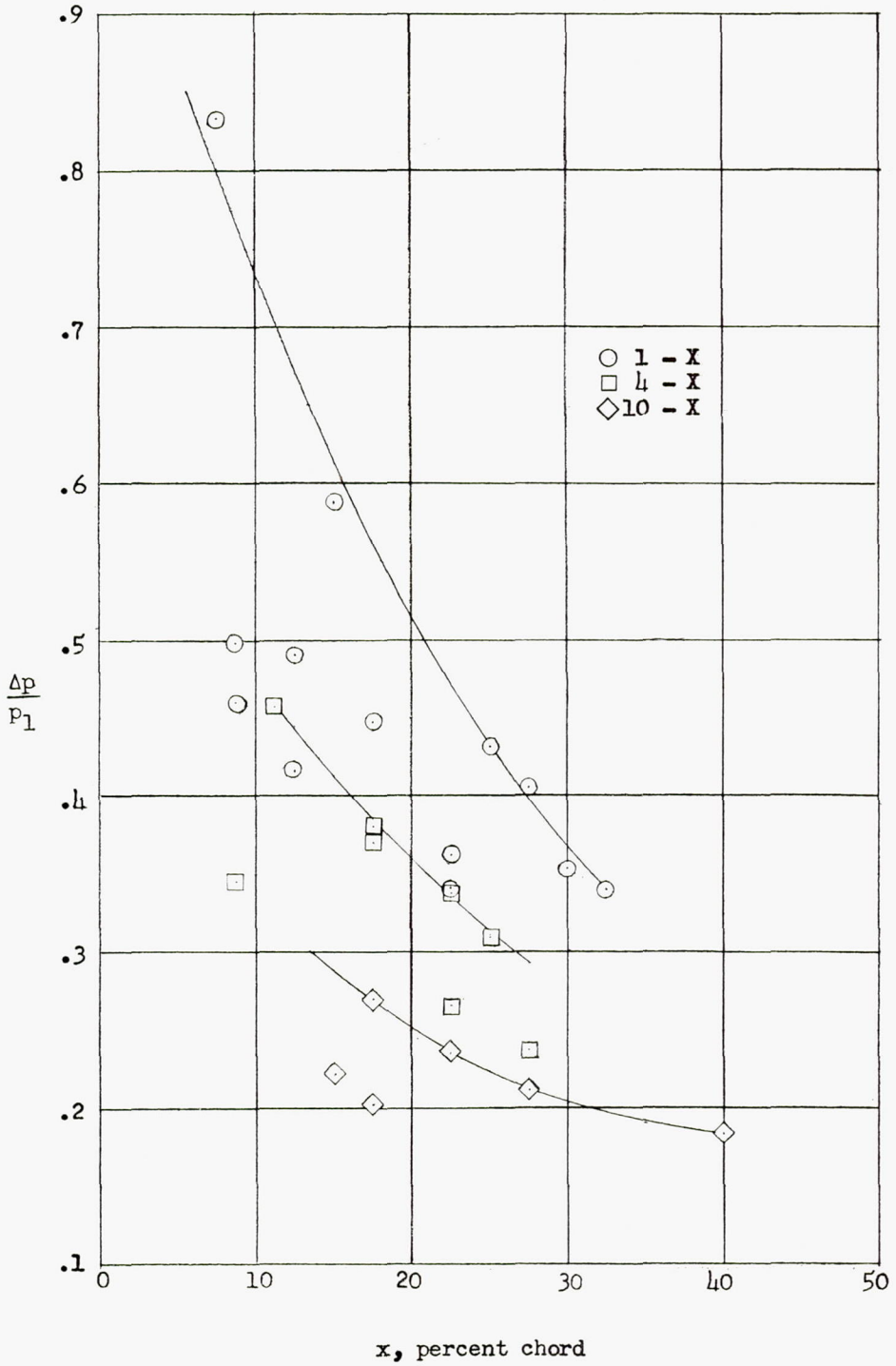


Figure 4.- The variation of pressure recovery with shock location along the flat plates at $\alpha = 0^{\circ}$.

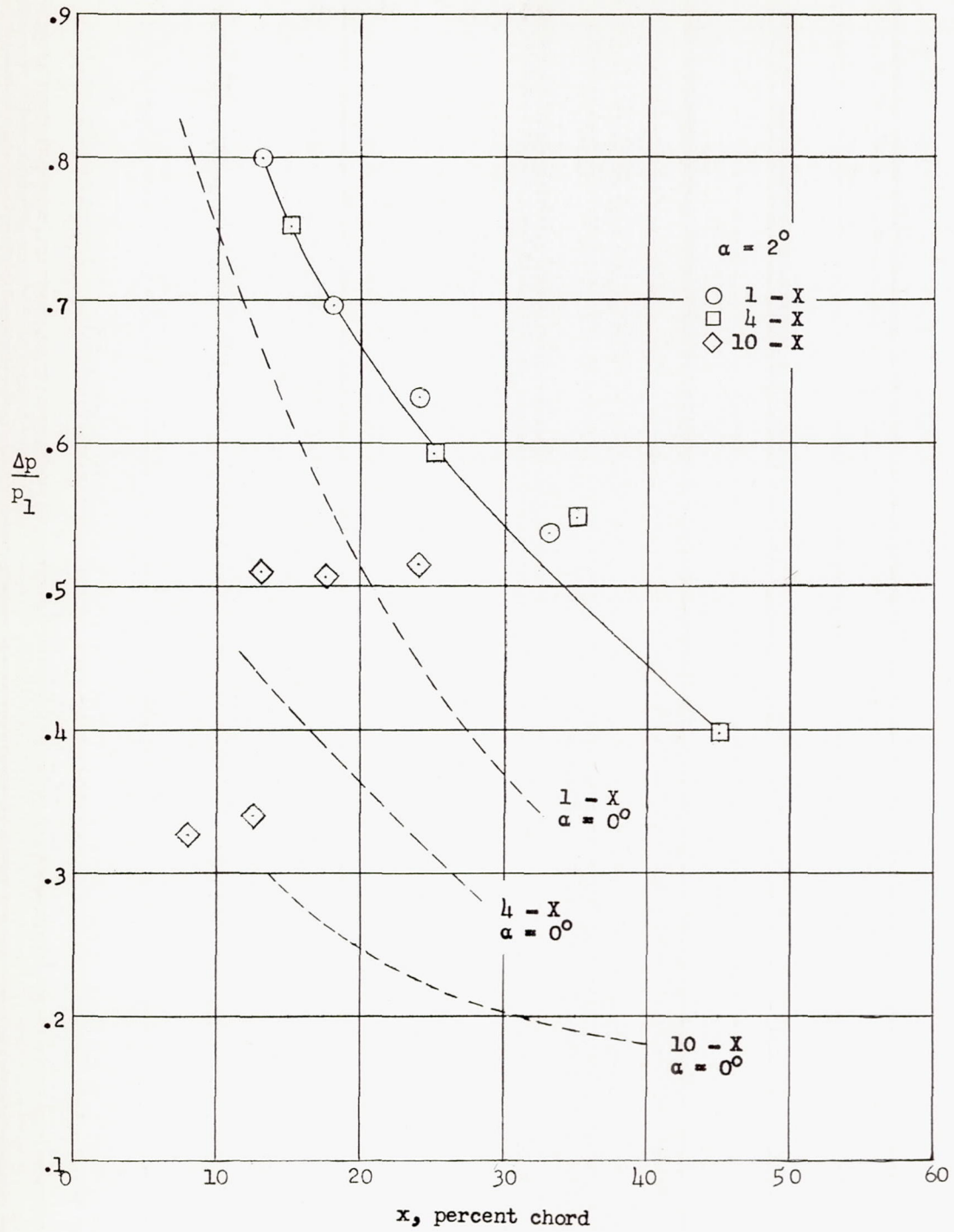


Figure 5.- The variation of pressure recovery with shock location along the flat plates for angles of attack of 0° and 2°.

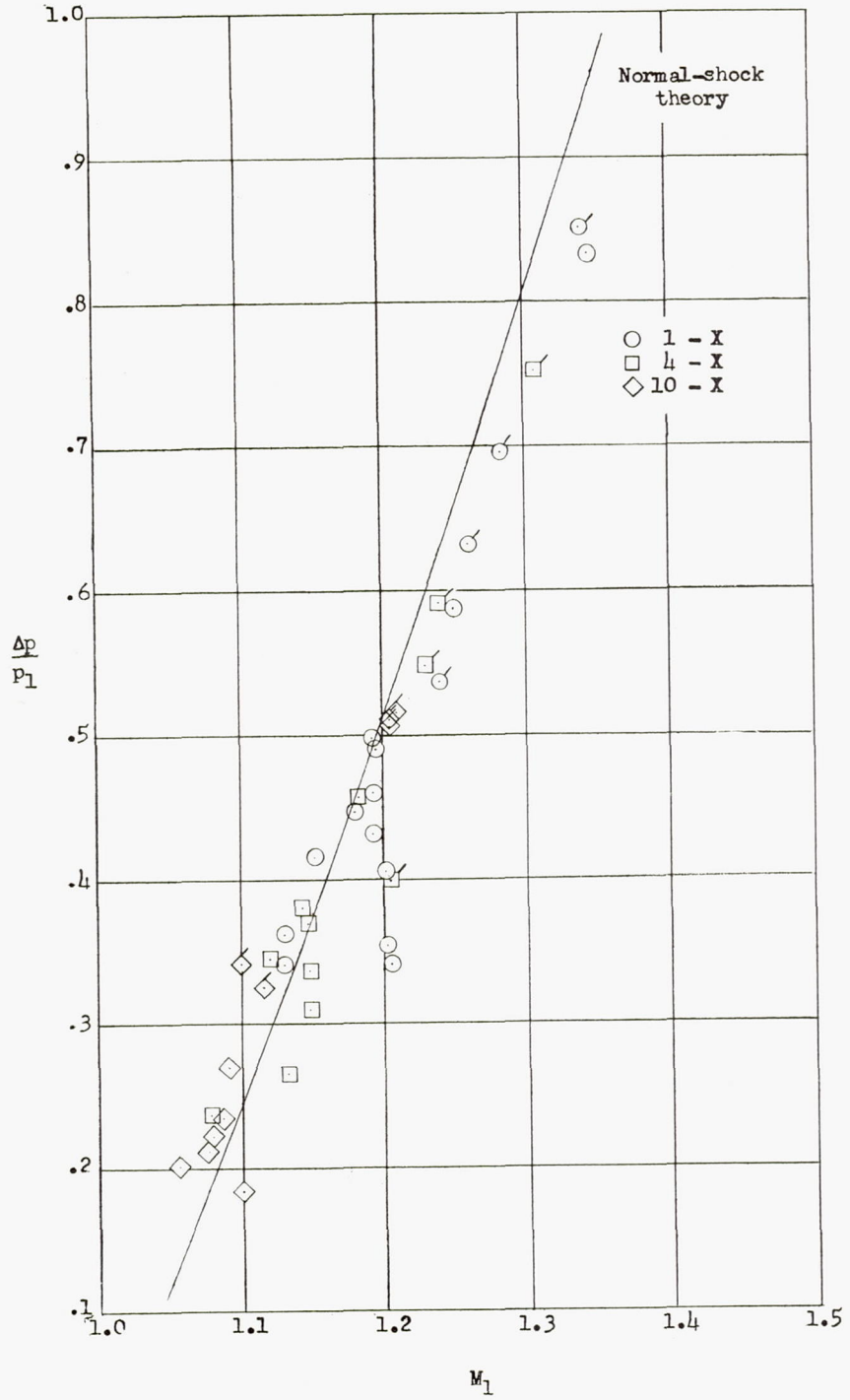


Figure 6.- Pressure recovery across shock on flat plates without separation. Flagged symbols are for $\alpha = 2^{\circ}$.

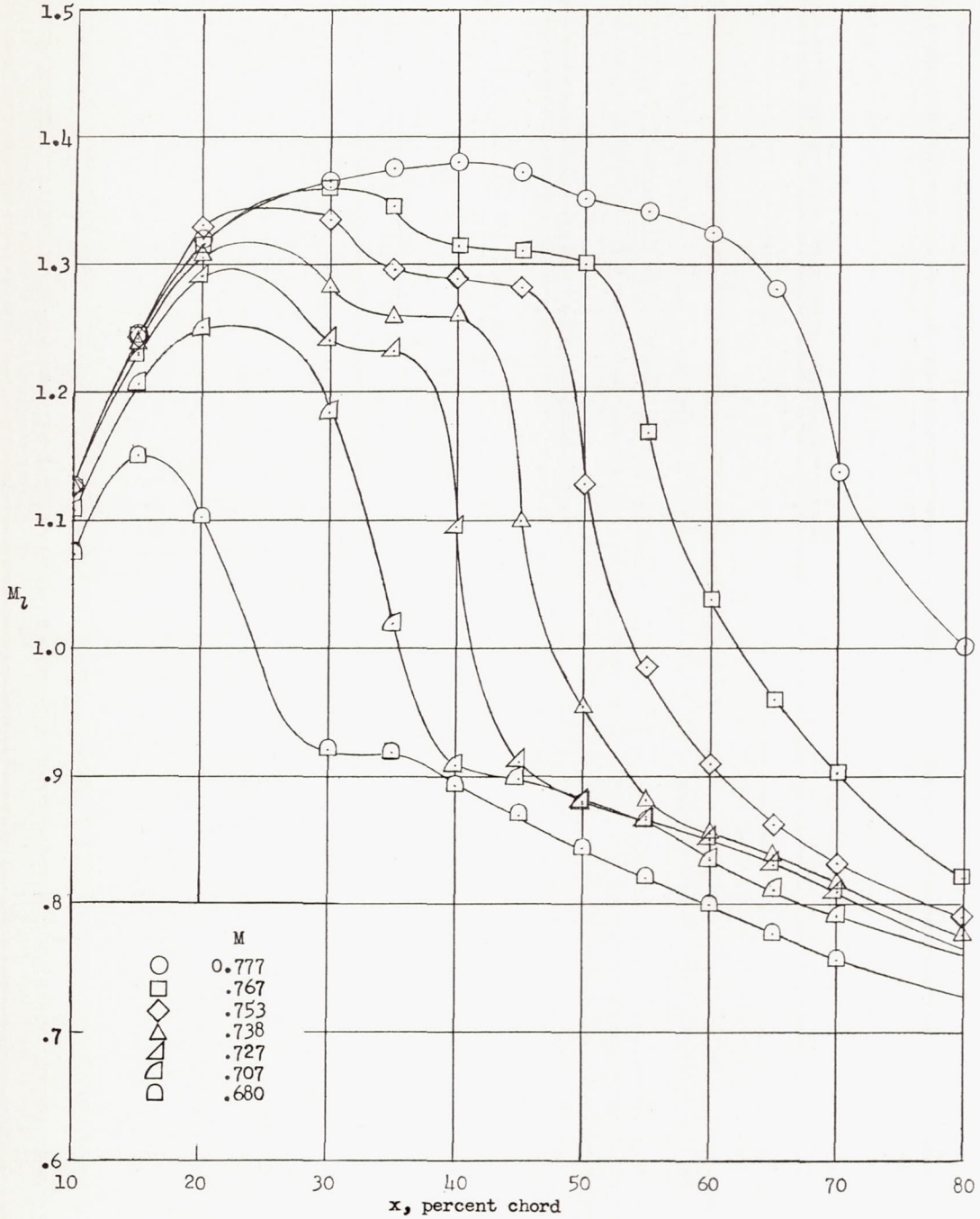


(a) Upper surface.

Figure 7.- Local Mach number distributions of an NACA 23015 airfoil at an angle of attack of $0^{\circ}$.

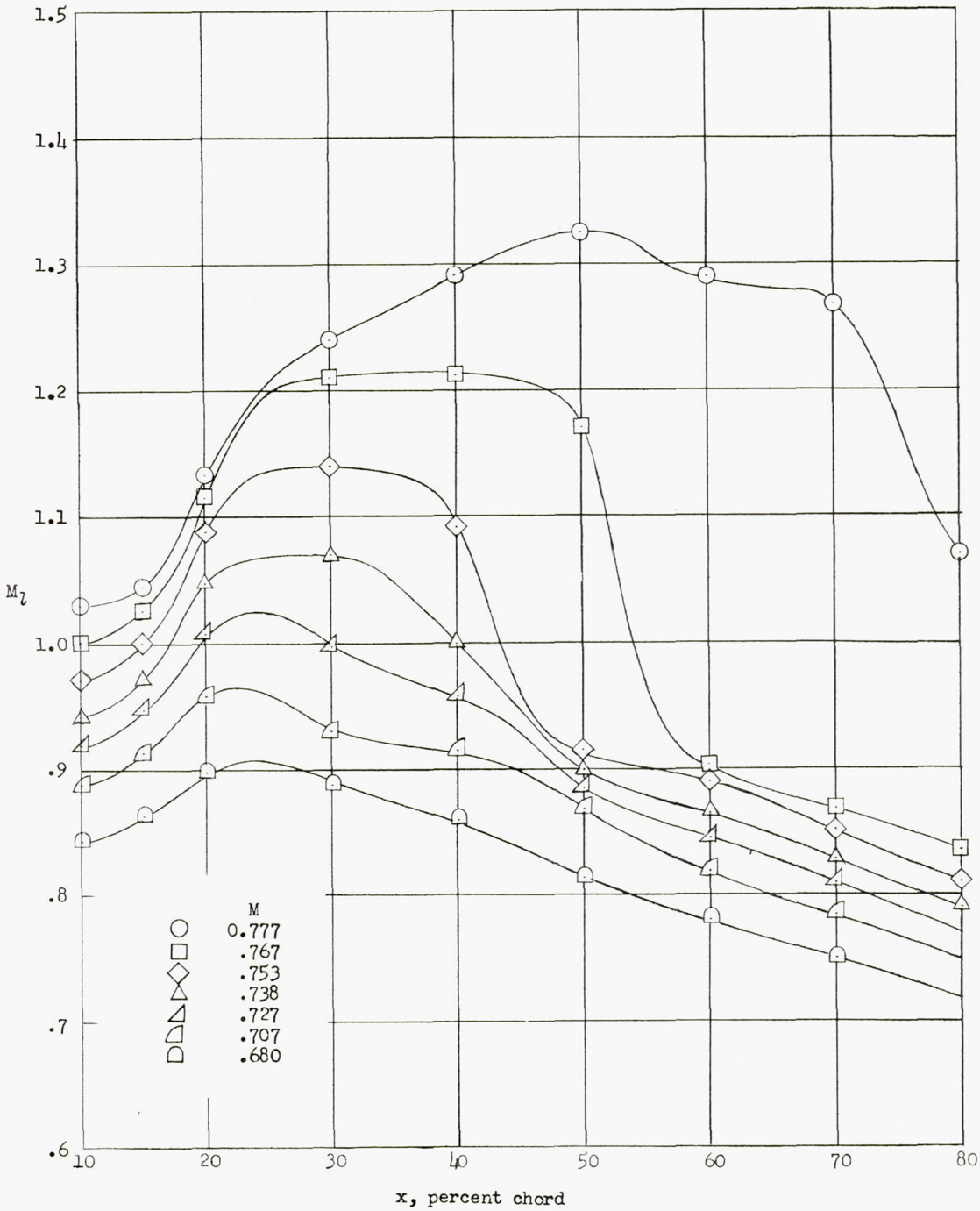


(b) Lower surface.

Figure 7.- Concluded.

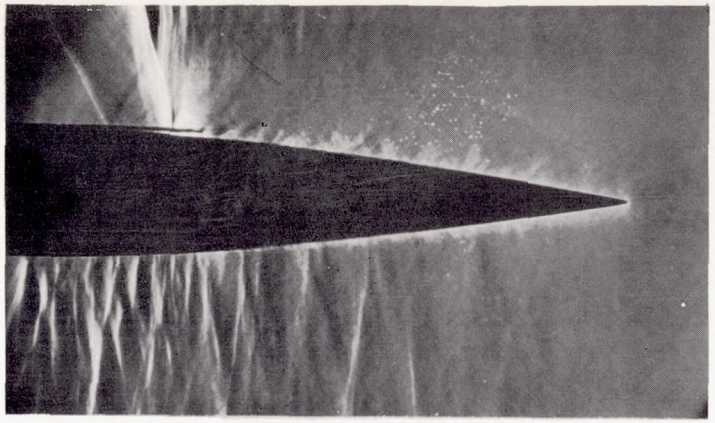

M = 0.742

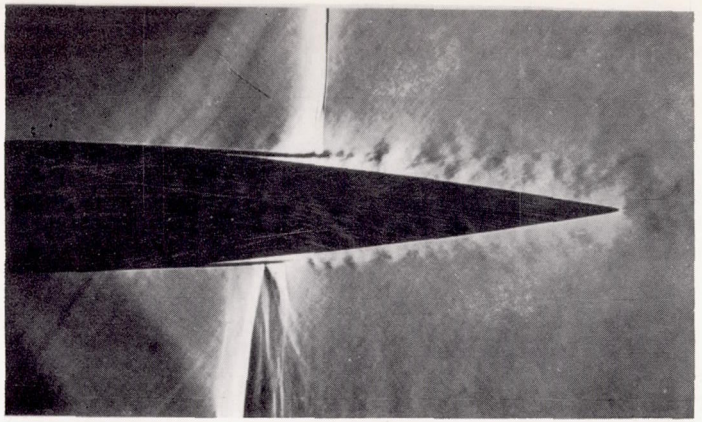

M = 0.769

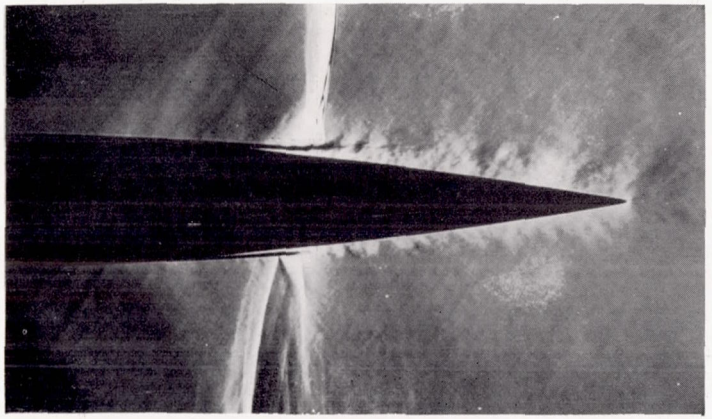

M = 0.774

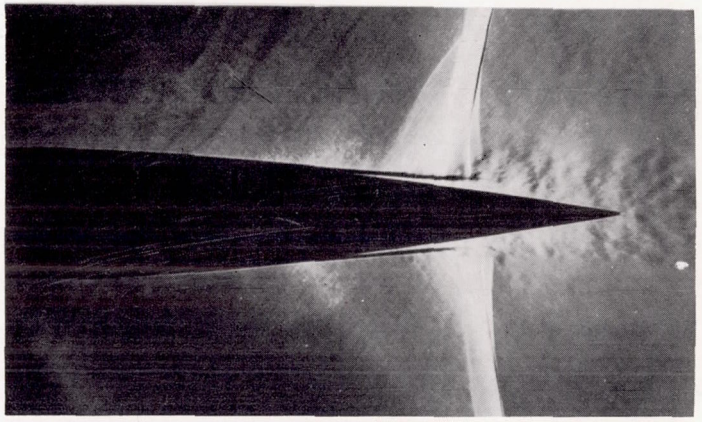

M = 0.780

L-93588

Figure 8.- Flow past the NACA 23015 airfoil; $\alpha = 0^{\circ}$.

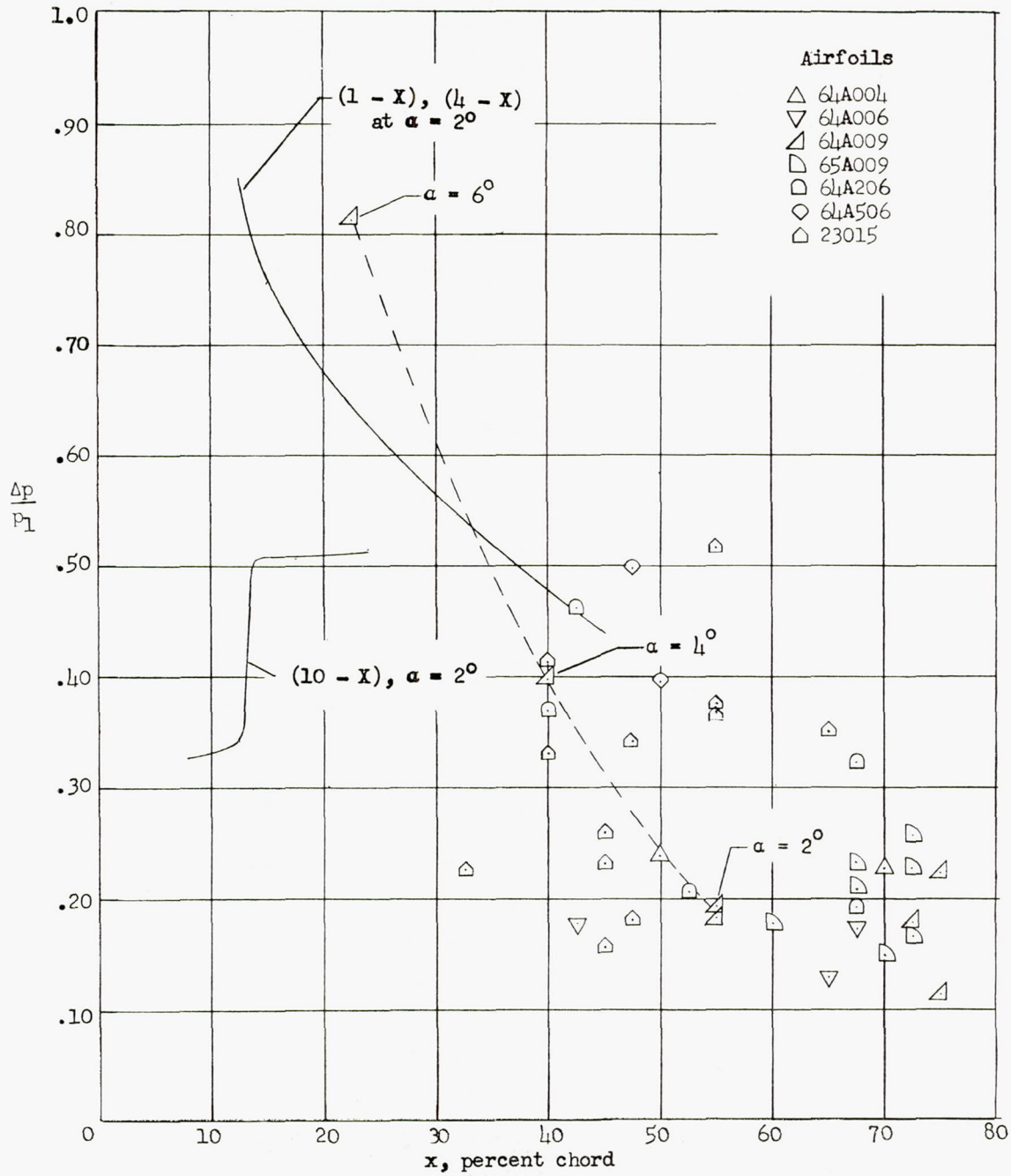


Figure 9.- Pressure recoveries on various NACA airfoils without separation.

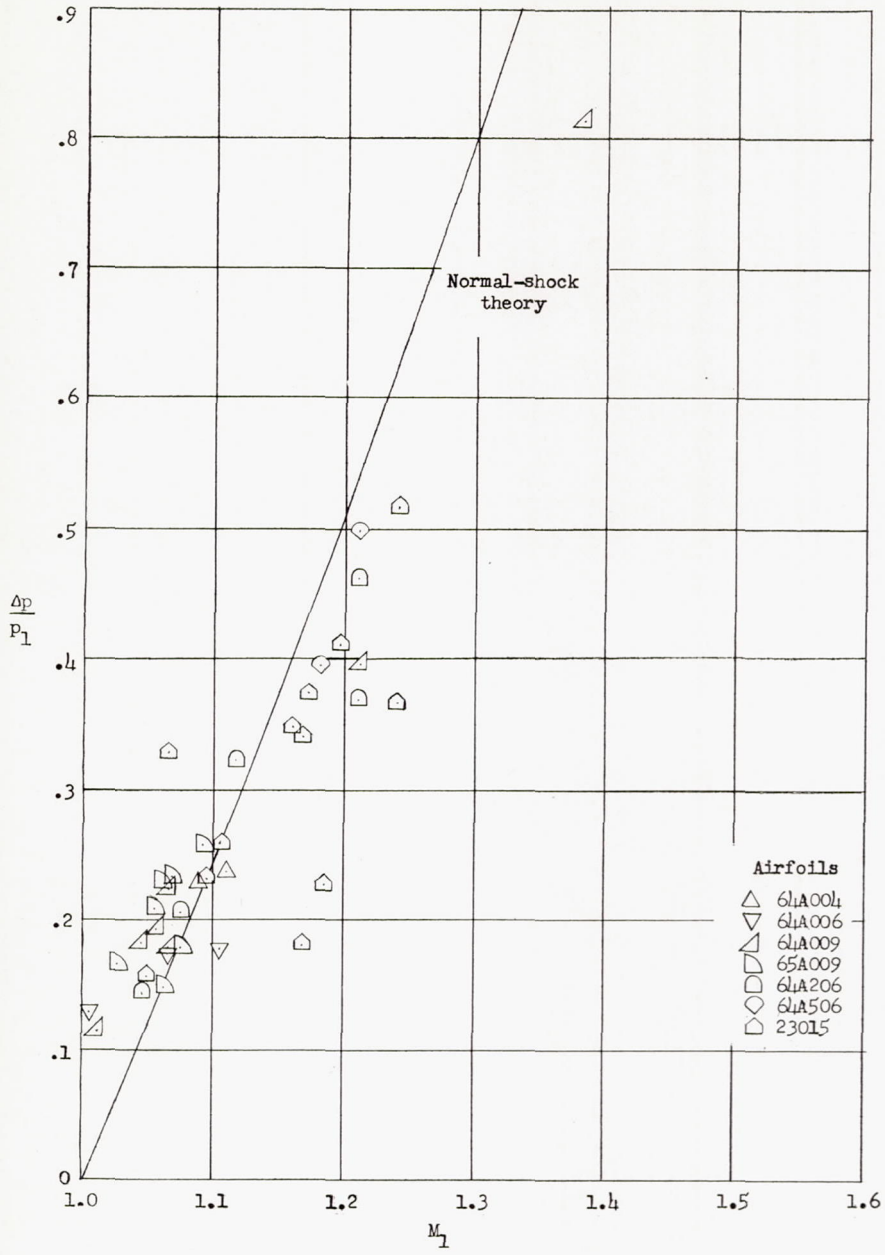


Figure 10.- A comparison of theoretical and experimental pressure recoveries across normal shocks on NACA airfoils without separation.